Hydrogen Evolution on Hydrophobic Aligned Carbon Nanotube Arrays

Abha Misra,[†] Jyotsnendu Giri,[‡] and Chiara Daraio[†,§,*]

[†]Graduate Aerospace Laboratories (GALCIT), [‡]Power, Environmental and Energy Research (PEER) Centre Division of Chemistry and Chemical Engineering, and [§]Applied Physics, California Institute of Technology, Pasadena, California 91125

ABSTRACT We investigate for the first time hydrophobic carbon nanotube-based electrochemical cells as an alternative solution to hydrogen sorting. We show that the electrically conducting surface of the nanotube arrays can be used as a cathode for hydrogen generation and absorption by electrolyzing water. We support our findings with Raman and gas chromatography measurements. These results suggest that carbon nanotube forests, presenting a unique combination of hydrophobicity and conductivity, are suitable for application in fuel cells and microelectromechanical devices.

KEYWORDS: hydrophobic carbon nanotubes · hydrogen sorting · water electrolysis · gas chromatography

Carbon nanotubes (CNTs) hydrophobic and hydrophilic properties have been receiving increasing attention in the scientific community. Such properties have been identified as important characteristics for a variety of practical applications, for example, for the fabrication of artificial lotus leaf-structures on cotton fabrics for self-cleaning in biomimicking systems,[1] in microelectromechanical systems (MEMS) to control spreading of liquids through the system,[2] and in cell-culture for the ability to absorb and preferentially distribute fluids (*i.e.*, wicking properties).[3]

From a fundamental standpoint, hydrophobicity is governed by the surface microstructure and surface energy.[4,5] In the particular case of CNTs, the ability to control their microstructure by controlling their growth parameters can provide means to improve their functionalities. For example, the vertical alignment of CNTs grown *via* thermal chemical vapor deposition processes was reported to induce anisotropy in their structural, mechanical, and electrical properties.[6] Coupling hydrophobicity with the anisotropic properties found in such forests of CNTs, could open doors to new applications including textiles, coating, sensing and biomechanical scaffolds. However, much of the potential provided by the hydrophobic property of vertically aligned CNTs is yet to be explored. Journet *et al.*,[7] studied the effect of fluid pressure on the stability of water droplets sitting on hydrophobic vertically aligned CNT forests. Their experiments showed that the CNT forests can withstand high excess pressure (larger than 10 kPa) without modifying the contact angle between the CNTs surface and the water droplet. Kakade *et al.* showed that CNTs can be switched from being hydrophobic to hydrophilic by applying a selected voltage,[8] suggesting CNTs as suitable candidates for electrochemical-based applications.[9,10]

Both free-standing single wall CNTs[11] and aligned multiwall CNTs[12] have been suggested as viable systems for hydrogen storage, either *via* electrochemical methods,[12] or *via* gas absorption methods at high pressure.[13]

The electro-decomposition of water using carbon electrodes has been proposed as a method for electrochemical storage of hydrogen.[14] Conductive vertically aligned CNT arrays can be suggested as alternative electrodes, offering the advantage of presenting an array of several thousand parallel probes (each corresponding to the individual CNTs in the forest). So far, the use of aligned CNTs in electrolytic application has been limited, as most of them are typically grown on semiconducting substrates that do not provide an efficient conduction pathway to be used as electrodes.

Here, we report for the first time an alternative solution to hydrogen sorting, by using the surface of dense vertical array of CNTs as a hydrophobic electrochemical cell for both generation and absorption of hydrogen. We take advantage of the conduc-

*Address correspondence to daraio@caltech.edu.

Received for review July 27, 2009 and accepted October 14, 2009.

Published online November 24, 2009.
10.1021/nn900878d CCC: $40.75

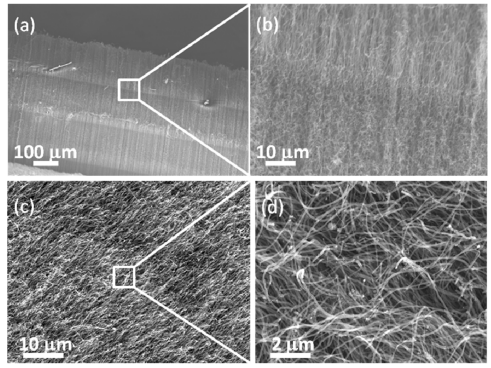

Figure 1. Scanning electron micrographs of a typical MWCNT forest used for our tests, showing the macroscopic nanotube alignment and the forest's characteristic microstructure: (a) low magnification image showing the vertical alignment across the entire forest's thickness (~800 μm), (b) higher magnification image showing the foamlike microstructure of the aligned CNTs, (c) top view of the surface of the aligned CNTs forest, (d) view of the nanotubes entanglement that provides surface connectivity and electrical pathways for high electrical conductivity.

tivity of the interconnected CNT forests and utilize their top surfaces as electrodes to study the effects of cathodic treatments with deionized water.

The aligned multiwalled carbon nanotubes (MWCNTs) considered for this study were produced by thermal chemical vapor deposition as described in the experimental section. Figure 1 panels a−d show scanning electron microscopy (SEM) images of the cross-section and top surface of our sample. Here the MWCNTs appear to be vertically aligned throughout the entire thickness of the forests (Figure 1a). The growth method used to prepare our samples was optimized to obtain clean surfaces, free from catalyst and amorphous carbon layers, without the need for any plasma or other treatment (see Figure 1c,d). SEM images taken at higher magnifications (Figure 1b,d) revealed a complex microstructure with MWCNTs rather entangled and cross-linked throughout the thickness, as well as along the surface of the samples.[6] Such multiscale structure, composed of vertically aligned bundles and individually entangled tube, gives the CNT forests unprecedented mechanical,[6] electrical,[6,15] and thermal responses.[16]

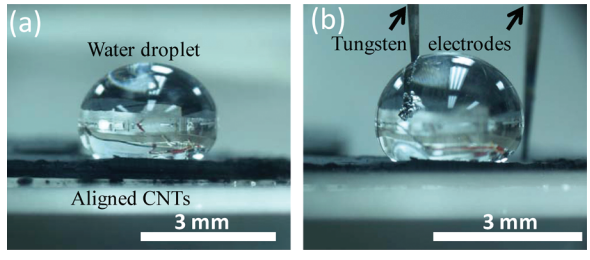

Figure 2. Digital micrographs of the deionized water droplet sitting on the hydrophobic surface of the CNT forest: (a) before testing, (b) during testing where oxygen bubbles are visible near the tungsten electrode (anode). The second tungsten needle, immersed in the CNTs forest farther away from the droplet, is visible in the background.

Typically, hydrophobic solids can achieve liquid−solid contact angles with water up to >120°. For the specific case of CNTs, it has been shown that taller arrays present a higher degree of hydrophobicity in comparison to short ones, probably related to a higher surface roughness resulting from the differences between the tubes' height.[17] We grew tall CNT forests (~800 μm) and found their surfaces exhibiting a highly hydrophobic behavior, in agreement with earlier investigations.[17] Figure 2a shows a digital micrograph of a water droplet (with a diameter of ~3 mm) resting on top of the CNTs surface. The static contact angle between the CNTs surface and the water droplet was measured to be as high as ~144°. This high contact angle observed on the CNT forests' surface could be explained by Wenzel's equation,[18] which relates the surface roughness with its hydrophobic property. The CNT forests used in our experiments presented an entangled "foamlike" microstructure (Figure 1) and somewhat "curled" CNT tips at the surface, which resulted in an increased roughness, likely responsible for the observed hydrophobic behavior. Below the surface, this entanglement created many small voids between bundles of CNTs. The air trapped in the voids could also provide support for sustaining the water droplet on the surface (Figure 2a).

Such ability to sustain individual water droplets on conductive CNT forests, suggested the possibility to utilize them to create novel electrochemical cells for hydrogen sorting. To test the electrochemical reactivity in our samples, we used a setup composed of two electrodes, as reported in ref. 19. For the assembly of the electrochemical cell, we immersed one of the electrodes (a micrometer-sharp metal tip connected to a power supply with positive polarity to function as an anode) in the deionized water droplet sitting on the top surface of vertically aligned CNTs (as shown in Figure 2b). We utilized the conducting surface of the CNTs as a cathode, with a given negative polarity provided by a tungsten needle inserted in the forest, as described in the schematic diagram in Figure 3. It is well-known that high electrode conductivity is important for electron transport during the electrochemical reaction. To verify this requirement in our MWCNT samples, we investigated the in-plane electrical properties of the as grown vertical arrays of CNTs. We performed DC measurements using a Cascade, M150 probe station, attached to Keithley-2635 source. The surface conductivity was measured to be 0.42 S cm^{-1} indicating that the MWCNTs are likely to be highly interconnected, and form continuous electrical paths along the sample's surface.

The same electronic system was used to trigger the electrochemical reaction in the water droplet. The experimental setup for the measurements is shown in Figure 3. It consisted of a main chamber with a two-way valve: one end of the valve was connected to vacuum pump to create a base pressure of 10^{-3} mbar, and the other end was connected to a vacuum sealed bag for

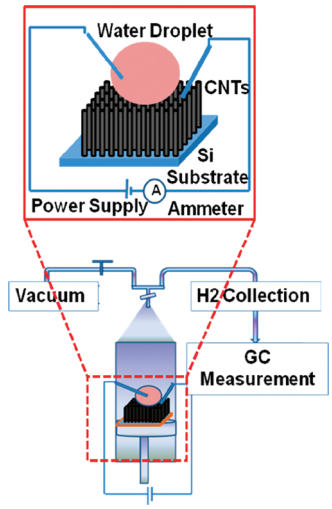

Figure 3. Schematic diagram showing the experimental set-up used for the electrolytic reaction measurements on the CNT forests. The top section shows an enlargement of the sample area, providing details on the probes positioning.

the collection of gases after the electrolytic reaction. The CNT sample was placed at the center of the chamber and connected to the two electrodes as shown in the detailed schematic on top of Figure 3.

Before testing, the system was vacuum purged to reduce the presence of atmospheric hydrogen in the tested sample. For the electrochemical reaction, an external voltage was applied across the two electrodes, causing an electrical current to flow through water droplet and the CNTs forest. It is well-known that in the process of electro-decomposition of water the amount of hydrogen produced is higher at lower operating voltages, but this implies a longer experimental time.[20] We chose to work with a voltage of −10 V to achieve faster kinetics. The electrical current was measured in the milliampere range (1−7 mA). As soon as the external voltage was applied, hydrogen evolution appeared near the surface of the CNTs and oxygen bubbles formed around the counter-tungsten electrode (see the movie included in the Supporting Information). During electrolysis, we did not observe any change in the surface characteristics and/or reduction of hydrophobicity of the CNT surfaces, differently from what was reported by Koratkar *et al.*[21]

RESULTS AND DISCUSSION

The electrochemical evolution of hydrogen can be described by the following reaction on the CNT surface (cathode):

$$H_2O(l) + 2e^- \rightarrow H_2(g) + 2OH^- \qquad (1)$$

The amount of hydrogen generated on the CNTs surface, calculated from the consumed charge during 1 h reaction,[22] was 2.6×10^{-4} gm. We performed gas chromatography (GC) measurements to quantify hydrogen evolution (see Methods). The results are reported in Figure 4. The amount of hydrogen collected during experiment was measured, $2.2 \pm 0.35 \times 10^{-5}$ gm. This value is lower than the amount calculated from the consumed charge, suggesting the possibility of hydrogen storage within the CNT forest. To verify the effectiveness of our CNTs as cathode for the electro-decomposition of water, we have repeated the same experiment replacing the CNTs by a hydrophobic paraffin film (a nonconductive material). To trigger the electrochemical reaction, we placed the two tungsten electrodes inside the water droplet. Interestingly, in this case no detectable hydrogen was found in the GC measurements, confirming the fast chemical reactivity of the vertically aligned CNT forests. This responsiveness may be attributed to the large surface area and/or catalytic activity of the CNTs, suggesting their potential use as highly efficient and fast systems for water decomposition.

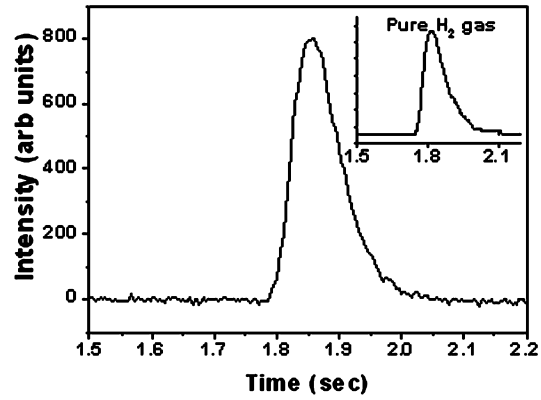

Figure 4. Typical chromatogram of hydrogen gas collected from the sample after performing the electrolysis of a water droplet on the hydrophobic CNTs surface. The inset shows the gas chromatogram of pure hydrogen, used for calibration.

High-resolution transmission electron microscopy (HRTEM) images of the as-grown MWCNTs used for this study are shown in Figure 5. The outer diameter of the CNTs ranged between ~15 nm (Figure 5a) and ~50 nm (Figure 5b). In these high-resolution images, the average distance between two neighboring carbon walls is 0.34 nm, which corresponds to the interlayer (002) d-spacing of the graphite lattice. Notably, a fraction of the as-grown CNT tips appeared to be completely open. Open CNT tips have been shown to allow hydrogen absorption in

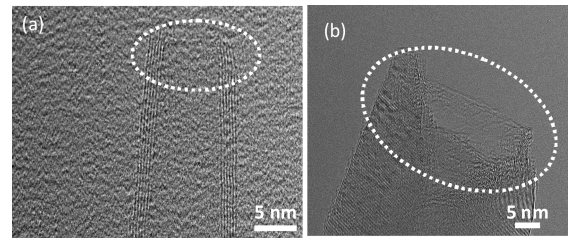

Figure 5. High resolution transmission electron microscopy (HRTEM) images: (a) TEM image of a multiwall CNT having ~15 nm outer diameter. It can be seen that the nanotube's tip is completely open (marked with a circle), (b) another open ended multiwall CNT (marked with a circle) with larger diameter (~50 nm).

the nanotubes' cores under both moderate[23] and ambient pressure conditions.[24] It is also plausible to expect physical and chemical absorption of hydrogen inside the bulk CNT forest, thanks to its characteristic foamlike microstructure (Figure 1). The open-ended CNT cores, the interwall spacing, and the intratube spacing in the dense forest all provide possible sites for hydrogen absorption. The CNT cores represent an ideal encapsulation area dominated by van der Waals' interactions between the carbon atoms and hydrogen molecules. Yang *et al.*,[25] have reported the interplanar spacing between adjacent graphene layers in MWCNTs as another possible adsorption sites for hydrogen. In our sample, the presence of open-ended tubes would provide an easier pathway for hydrogen to enter the interspaces between graphene layers. The possibility for hydrogen absorption in the CNTs' cores and in the interwall spacing is also supported by the numerical analysis performed by Kang *et al. via* DFT calculations.[26] The controlled enhancement of the ability to store hydrogen in our hydrophobic CNT forests *via* chemical routes will be a matter of future investigations.

Raman spectroscopy measurements were performed to elucidate the hydrogenation of the CNTs after water electrolysis. Figure 6 panels a−c indicate typical Raman spectra obtained from a CNT sample before and after performing water electrolysis on its hydrophobic surface. The Raman spectrum has three bands. The high energy Raman band, at ~1570 cm^{-1}, is called the tangential mode (G-band), which is related to the graphite E_{2g} symmetric mode. The D-band (~1350 cm^{-1}) is induced by the presence of defects. The strongest peak in the second order spectrum is the overtone of the D band at ~2700 cm^{-1}, which is called G′-band.[27] The intensity of both the G-band and the D-band depends on the concentration of defects in the sample. In an earlier investigation on boron-doped CNTs, the absolute intensities of the G- and G′-bands were reported to decrease with the increase of defect concentration.[28] A similar behavior has been observed in our measurements, as reported in Figure 6a. The absolute intensities of the G and G′ bands decrease, and it is evident from the observed spectra that the intensity decrease in the G′-band is more rapid than that of the G-band. This is because the G′-band is strongly influenced by the enhancement of defect concentration. A large defect concentration might lead to an increased scattering cross section for the defect-induced Raman mode.

The change in spectral frequency (at maximum intensity) of the G-band after electrolysis was up-shifted by 3 cm^{-1}. Such a shift suggests that the van der Waals attraction between the hydrogen and the carbon nanotube is increased, which in turns increases the energy necessary for vibrations to occur. This is reflected in the higher frequency of the Raman peaks.[29] The intensity ratio (I_D/I_G) and the measurement of the Full Width at Half-Maximum (FWHM) of the deconvoluted D-band and G-band provide an estimate of the degree of graphitization of the CNT walls. Table 1 summarizes the relative Raman peak

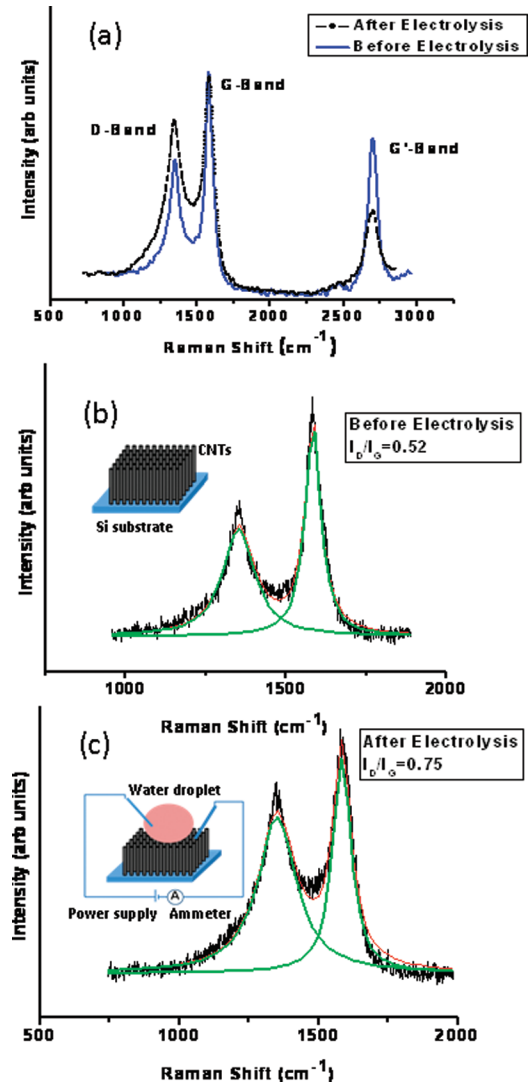

Figure 6. Raman spectroscopy results: (a) comparison of the overall spectra obtained from a CNT sample before (solid line) and after (dotted line) performing the electrolysis experiment, (b) Lorentzian fitted spectrum showing the comparative D and G bands before electrolysis, (c) Lorentzian fitted spectra showing comparative D and G bands after electrolysis.

intensities and FWHM values, before and after electrolysis. After electrolysis, the I_D/I_G of these pristine MWCNTs increased from 0.52 to 0.75 (Figure 6b,c), which shows a lower degree of graphitization related to the generation of defects. The FWHM value of the deconvoluted D-band after electrolysis was increased by 80.5 cm^{-1}, the G-band increased by 17.5 cm^{-1}, and G′-band by 44.4 cm^{-1} (see

TABLE 1. Comparison of the spectral parameters in the Raman measurements, before and after electrolysis; the I_D/I_G ratios, and the FWHM for the D-Band, G-Band and G′-Band

	I_D/I_G	D-band FWHM (cm^{-1})	G-band FWHM (cm^{-1})	G′-band FWHM (cm^{-1})
before electrolysis	0.52	149.3	60.0	75.8
after electrolysis	0.75	229.8	77.5	120.2

Table 1). The significant increase in I_D/I_G and FWHM values are an indication of hydrogen absorption.[30] This can be related to the possible physical absorption of hydrogen inside the core and interwall spacing of CNTs, or to chemisorption induced by the applied potential.

CONCLUSION

We investigated the applicability of the hydrophobic surface of as-grown aligned multiwalled carbon nanotube forests as electrochemical cells for the electrodecomposition of water. We reported hydrogen generation on the carbon nanotube surfaces when used as cathodes in the reaction. Raman and gas chromatography investigations demonstrated the possibility of reversible hydrogen absorption in the bulk of the carbon nanotube forests and inside the MWCNTs. This unique combination of high hydrophobicity and high conductivity of the carbon nanotube forests has shown potential for use in highly efficient compact fuel cells and MEMS applications.

METHODS

Growth of Vertically Aligned Multiwalled Carbon Nanotubes. Aligned nanotubes were grown *via* chemical vapor deposition using a two-stage thermal CVD system. This system consists of a quartz tube of 30 mm in diameter, and 1000 mm long, having a 200 mm preheating and a 500 mm heating zone. The temperature controllers were set to desired temperatures (80 °C for preheating zone and 825 °C for heating zone). SiO_2 was used as a substrate for growth. A mixture of Fe-catalyst (ferrocene) and carbon source (toluene) (0.02 g/mL) was injected into the preheating zone at the rate of 5 mL/15 min. A flow of 800 SCCM of argon gas was maintained as a carrier for the gas solution that was fed into the heating zone. The outer diameter of the grown CNTs ranged from 15 to 50 nm and their length was ~800 μm.

Gas Chromatography (GC). The hydrogen concentration was analyzed on a carbon-based molecular sieve column (Agilent Molsiv 5A 30 m × 0.320 mm ID) with a thermal conductivity detector (TCD). A Hewlett-Packard 5890 GC was operated for 0.3 min, at which point the injector was purged with a split flow of 20 mL/min. Ultrahigh purity nitrogen was used as a carrier gas, and the oven temperature was kept isothermal at 200 °C. Injections of 10−1000 μL were performed manually with a gastight syringe. The hydrogen concentration in the gas samples (after electrolysis) was determined from the calibration curve, generated by injecting different volumes (10−1000 μL) of ultra pure (99.99%) hydrogen.

Acknowledgment. We acknowledge funding from the Army Research Office, Institute for Collaborative Biotechnologies (ICB) for support of this project. This work benefited from use of the Caltech Environmental Analysis Centre (EAS), GC/MS facility. We thank Dr. N. F. Dalleska for helpful discussions.

Supporting Information Available: The digital movie-clip captured during experiments shows water electrolysis on the hydrophobic carbon nanotubes surface. The hydrogen evolution can be seen to be bubbling from the CNT cathode surface, and oxygen bubbles evolve at the anode. This material is available free of charge *via* the Internet at http://pubs.acs.org.

REFERENCES AND NOTES

1. Liu, Y.; Tang, J.; Wang, R.; Lu, H.; Li, L.; Kong, Y.; Qi, K.; Xin, J. H. Artificial Lotus Leaf Structures from Assembling Carbon Nanotubes and Their Applications in Hydrophobic Textiles. *J. Mater. Chem.* **2007**, *17*, 1071–1078.
2. Doms, M.; Feindt, F.; Kuipers, W. J.; Shewtanasoontorn, D.; Matar, A. S.; Brinkhues, S. R.; Welton, H.; Mueller, J. Hydrophobic Coating for MEMS Applications. *J. Micromech. Microeng.* **2008**, *18*, 055030–055042.
3. Lee, J. E.; Khang, D.; Kim, Y. E.; Webster, T. Stem Cell Impregnated Carbon Nanofibers/Nanotubes for Healing Damaged Neural Tissue. *J. Mater. Res. Soc. Symp. Proc.* **2006**, 915.
4. Oner, D.; McCarthy, T. J. Effects of Topography Length Scales on Wettability. *Langmuir* **2000**, *16*, 7777–7782.
5. Li, H. J.; Wang, X. B.; Song, Y. L.; Liu, Y. Q.; Li, Q. S.; Jiang, L.; Zhu, B. D. Super-Amphiphobic Aligned Carbon Nanotube Films. *Angew. Chem., Int. Ed.* **2001**, *40*, 1743–1746.
6. Misra, A.; Greer, J. R.; Daraio, C. Strain Rate Effects in the Mechanical Response of Polymer-Anchored Carbon Nanotube Foams. *Adv. Mater.* **2008**, *20*, 1–5.
7. Journet, C.; Moulinet, S.; Ybert, C.; Purcell, S. T.; Bocquet, L. Contact Angle Measurements on Superhydrophobic Carbon Nanotube Forests: Effect of Fluid Pressure. *Europhys. Lett.* **2005**, *71*, 104–109.
8. Kakade, B.; Mehta, R.; Durge, A.; Kulkarni, S.; Pillai, V. Electric Field Induced, Superhydrophobic to Superhydrophilic Switching in Multiwalled Carbon Nanotube Papers. *Nano Lett.* **2008**, *8*, 2693–2696.
9. Gooding, J. J. Nanostructuring Electrodes with Carbon Nanotubes: A Review on Electrochemistry and Applications for Sensing. *Electrochim. Acta* **2005**, *50*, 3049–3060.
10. Wildgoose, G. G.; Banks, C. E.; Leventis, H. C.; Compton, R. G. Chemically Modified Carbon Nanotubes for Use in Electroanalysis. *Microchim. Acta* **2006**, *152*, 187–214.
11. Liu, C.; Fan, Y. Y.; Liu, M.; Comg, H. T.; Chengand, H. M.; Dresselhaus, M. S. M.S. Hydrogen Storage in Single-Walled Carbon Nanotubes at Room Temperature. *Science* **1999**, *286*, 1127–1129.
12. Hao, D.; Zhu, H.; Zhang, X.; Li, Y.; Xu, C.; Mao, Z.; Liu, J.; Wu, D. Electrochemical Hydrogen Storage of Aligned Multi-Walled Carbon Nanotubes. *Chin. Sci. Bull.* **2008**, *48*, 538–542.
13. Dillion, A. C. C.; Jones, K. M.; Bekkedahl, T. A.; Kiang, C. H.; Bethune, D. S.; Heben, M. J. Storage of Hydrogen in Single-Walled Carbon Nanotubes. *Nature* **1997**, *386*, 377–379.
14. Jurewicz, K.; Frackowiak, E.; Beguin, F. Enhancement of Reversible Hydrogen Capacity into Activated Carbon through Water Electrolysis. *Electrochem. Solid-State Lett.* **2001**, *4*, A27–A29.
15. White, C. T.; Todorov, T. N. Carbon Nanotubes As Long Ballistic Conductors. *Nature* **1998**, *393*, 240–242.
16. Che, J.; Cagin, T.; Goddard, W. A. Thermal Conductivity of Carbon Nanotubes. *Nanotechnology* **2000**, *11*, 65–69.
17. Lau, K. K. S.; Bico, J.; Teo, K. B. K.; Chhowalla, M.; Amaratunga, G. A. J.; Milne, W. I.; McKinley, G. H.; Gleason, K. K. Superhydrophobic Carbon Nanotube Forests. *Nano Lett.* **2003**, *3*, 1701–1705.
18. Wenzel, R. N. Resistance of Solid Surfaces to Wetting by Water. *Ind. Eng. Chem.* **1936**, *28*, 988–994.
19. Tzeng, Y.; Chen, Y.; Sathitsuksanoh, N.; Liu, C. Electrochemical Behaviors and Hydration Properties of Multi-Wall Carbon Nanotube Coated Electrodes in Water. *Diamond Relat. Mater.* **2004**, *13*, 1281–1286.
20. Seehra, M. S.; Ranganathan, S.; Manivannan, A. Carbon-Assisted Water Electrolysis: An Energy-Efficient Process to Produce Pure H2 at Room Temperature. *Appl. Phys. Lett.* **2007**, *90*, 044104.
21. Wang, Z.; C., L.; Chen, L.; Nayak, S.; Ajayan, P. M.; Koratkar, N. Electrochemically Controlled Transport of Water through Carbon Nanotube Membranes. *Nano Lett.* **2007**, *7*, 697–702.

22. Souza, R. F. de; Padilha, J. C.; Goncalves, R. S.; Souza, M. O. de; Berthelot, J. R. Electrochemical Hydrogen Production from Water Electrolysis Using Ionic Liquid As Electrolytes: Towards the Best Device. *J. Power Sources* **2007**, *164*, 792–798.
23. Chen, Y.; Shaw, D. T.; Bai, X. D.; Wang, E. G.; Lund, C.; Lu, W. M.; Chung, D.D. L. Hydrogen Storage in Aligned Carbon Nanotubes. *Appl. Phys. Lett.* **2001**, *78*, 2128–2130.
24. Jang, J. W.; Lee, C. E.; Oh, C. I.; Lee, C. J. Hydrogen Storage Capacity of Different Carbon Nanostructures in Ambient Conditions. *J. Appl. Phys.* **2005**, *98*, 074316–074319.
25. Yang, Q. H. Surface, Pore Structure of Carbon Nanotubes and Its Influence on Hydrogen Storage. Post Ph.D. Report. Chinese Academy of Sciences, Institute of Metal Research, 2001.
26. Han, S. S.; Kim, H. S.; Han, K. S.; Lee, J. Y.; Woo, S. I.; Duin, A.C. T.; Goddard, W. A.; Kang, J. K. Nanopores of Carbon Nanotubes As Practical Hydrogen Storage Media. *Appl. Phys. Lett.* **2005**, *87*, 213113–213116.
27. Saito, R.; Grüneis, A.; Samsonidze, Ge. G.; Brar, V. W.; Dresselhaus, G.; Dresselhaus, J., M.S. A.; Cançado, L. G.; Fantini, C.; Pimenta, M. A.; Souza Filho, A. G. Double Resonance Raman Spectroscopy of Single-Wall Carbon Nanotube. *New J. Phys.* **2003**, *5*, 157–172.
28. Maultzsch, J.; Reich, S.; Thomsen, C.; Webster, S.; Czerw, R.; Carroll, D. L.; Vieira, S. M.; Birkett, C. P. R.; Rego, C. A. Raman Characterization of Boron-Doped Multiwalled Carbon Nanotubes. *Appl. Phys. Lett.* **2002**, *81*, 2647–2650.
29. Sinani, V. A.; Gheith, M. K.; Yaroslavov, A. A.; Rakhnyanskaya, A. A.; Sun, K.; Mamedov, A. A. Aqueous Dispersions of Single-Wall and Multiwall Carbon Nanotubes with Designed Amphiphilic Polycations. *J. Am. Chem. Soc.* **2005**, *127*, 3463–3472.
30. Nguyen, K. T.; Shim, M. Role of Covalent Defects on Phonon Softening in Metallic Carbon Nanotubes. *J. Am. Chem. Soc.* **2009**, *131*, 7103–7106.